Report

Current Biology

Invasive golden oyster mushrooms are disrupting native fungal communities as they spread throughout North America

Graphical abstract

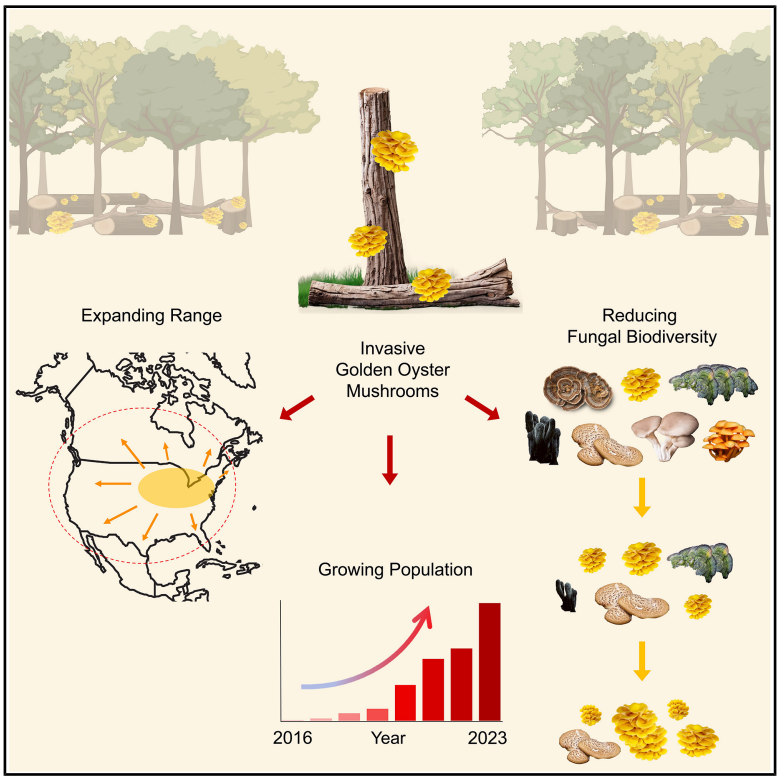

Authors

Aishwarya Veerabahu, Mark T. Banik, Daniel L. Lindner, Anne Pringle, Michelle A. Jusino

Correspondence

veerabahu@wisc.edu (A.V.), michellejusino@gmail.com (M.A.J.)

In brief

The impacts of invasive fungi on ecosystems are rarely documented, but non-native mushrooms are often moved to new regions via global trade. Veerabahu et al. show the widely cultivated escapee, the golden oyster mushroom, is changing native fungal biodiversity as it invades. GOM has spread rapidly in North America and will continue expanding its range.

Highlights

- Invasive golden oyster mushrooms (GOMs) are displacing native fungal communities
- In forests, trees with GOM house fewer fungi as compared with trees without GOM
- As of now, GOM is found in 25 US states and one Canadian province
- Climate change may enable GOM to spread more widely

Veerabahu et al., 2025, Current Biology *35*, 3994–4002
August 18, 2025
https://doi.org/10.1016/j.cub.2025.06.049

CellPress

CellPress

Current Biology

Report

Invasive golden oyster mushrooms are disrupting native fungal communities as they spread throughout North America

Aishwarya Veerabahu,[1,2,5,*] Mark T. Banik,[2] Daniel L. Lindner,[2] Anne Pringle,[1,3] and Michelle A. Jusino[2,4,*]
[1]Department of Botany, University of Wisconsin-Madison, Madison, WI 53706, USA
[2]Center for Forest Mycology Research, Northern Research Station, USDA Forest Service, Madison, WI 53726, USA
[3]Department of Bacteriology, University of Wisconsin-Madison, Madison, WI 53706, USA
[4]School of Forest, Fisheries, and Geomatics Sciences, University of Florida, Gainesville, FL 32611, USA
[5]Lead contact
*Correspondence: veerabahu@wisc.edu (A.V.), michellejusino@gmail.com (M.A.J.)
https://doi.org/10.1016/j.cub.2025.06.049

SUMMARY

Earth's biodiversity is in decline, and invasive species are among the greatest threats to local ecosystems.[1] While the impacts of invasive plants, animals, and pathogens are increasingly well documented, the impacts of invasive nonpathogenic microbes are not.[2–4] The golden oyster mushroom (GOM; *Pleurotus citrinopileatus*) is a white-rot wood decay fungus and grows primarily on hardwoods.[5–7] GOM is a widely cultivated and prized edible fungus native to eastern Asia. GOM was imported into North America in the early 2000s and is now sold in popular mushroom-growing kits. GOM escaped into North American forests around 2010[7,8] and is now rapidly expanding its range. We predicted GOM is changing fungal community composition and lowering species richness in the wood it colonizes. We conducted a field survey of fungal communities from dead elm trees in south-central Wisconsin, USA, and generated metabarcoding data to determine whether fungal communities and species richness differ when GOM is present. To contextualize GOM's impacts, we used community science observations of GOM in North America to map GOM's range expansion and modeled its potential future distribution. When GOM is present, fungal community composition significantly changes, and fungal species richness significantly decreases. GOM has spread quickly and widely in just 8 years, and it is now found in 25 states and 1 Canadian province. While GOM currently grows in middle and northeastern North America, our model predicts climate change will make many other parts of the continent climatically suitable, and GOM will likely continue its range expansion.

RESULTS

Survey data reveal which trees have GOM

To catalog the biodiversity of fungi in trees with or without golden oyster mushrooms (GOMs; *Pleurotus citrinopileatus* Singer [Agaricales, Basidiomycota]), we sampled 26 dead elm (*Ulmus* spp.) trees, 13 with GOM basidiocarps and 13 without GOM basidiocarps (Figure 1). Wood shavings were sterilely drilled from each of three different heights on each of the 26 trees, resulting in 78 wood samples for metabarcoding. The resulting data of the 78 wood samples were either analyzed independently or combined by tree for a tree-level analysis. From this point forward, we use the word "wood" to reference the data processed as individual samples and "tree" to reference the data combined by tree. The indexed metabarcoding samples generated a range of 16,274–146,889 (average 72,763) reads, representing 1–65 (average 13) operational taxonomic units (OTUs)[9] per sample and encompassing 321 OTUs in total. We recovered three (of three) species included in our positive biological mock community, confirming the detectability of a subset of fungi we predicted might be in our samples. We recovered 12 (of 12) of our synthetic mock community (SynMock[10]), confirming the accuracy of our amplification protocols and bioinformatics parameters.

Basidiocarps were an imperfect predictor of GOM absence. Metabarcoding data revealed the presence of GOM in two trees without GOM basidiocarps. Because fungi often exist as mycelia hidden within substrates, our result is not surprising. In addition, one tree with GOM basidiocarps at its base did not return any reads of GOM. Either the fungus had not reached the heights we sampled, or the fungus was missed in our drilling or molecular processing. Finally, seven of the 15 GOM trees were apparently not fully colonized by GOM. In these trees, we only detected GOM in one or two of the three sampled heights. Heights with GOM were different among the seven trees. For example, one tree only had GOM detected at a height of 0.3 m, while another tree only had GOM detected at 2.7 m (Figure S1). We subsequently defined a tree "with GOM" as a tree from which we found GOM basidiocarps *or* detected DNA sequences matching GOM. Using this definition, 15 of the 26 surveyed trees were defined as trees with GOM. Although our sample size was

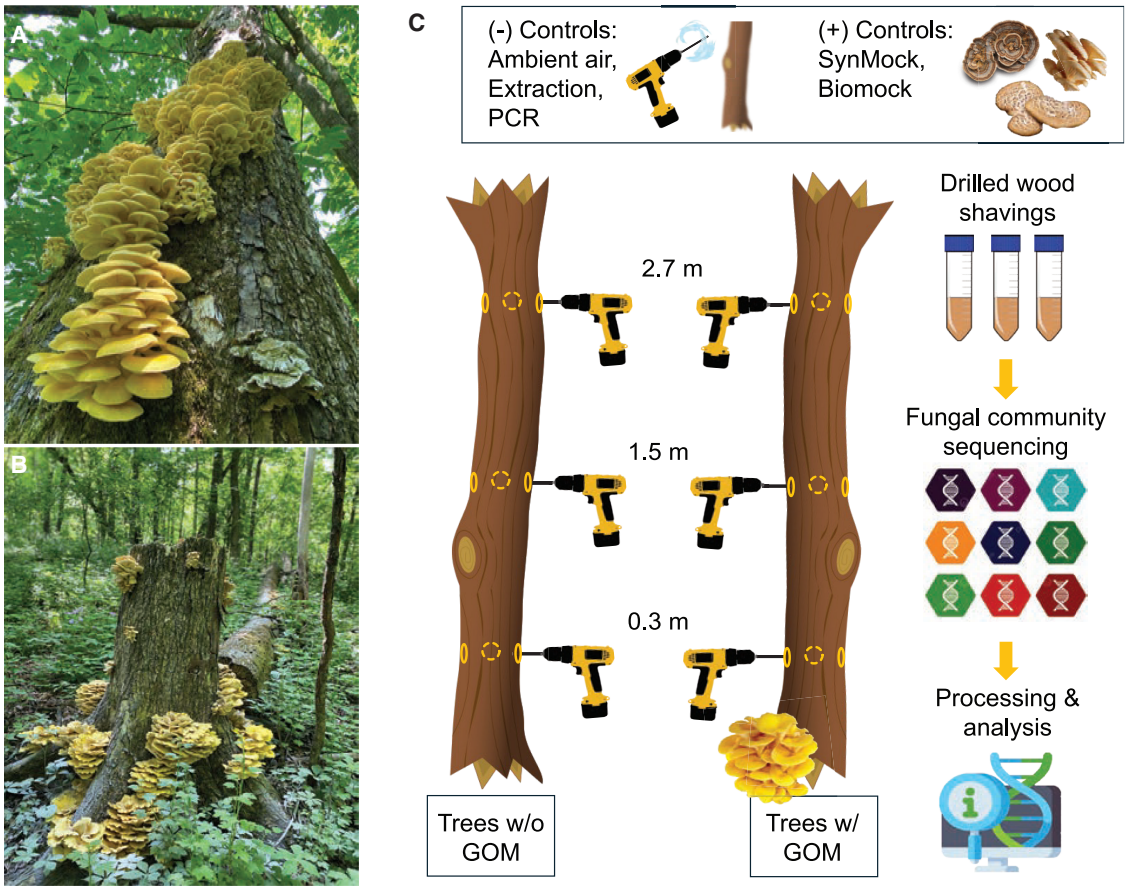

Figure 1. Basidiocarps of invasive GOMs and sampling scheme

(A) Clusters of GOM growing abundantly along a standing dead snag.

(B) GOM growing on both halves of a snapped dead elm, and trees with GOM are often broken. Note white spores on foliage under basidiocarps. Photographs by Aishwarya Veerabahu.

(C) Schematic visualizing our field survey sampling methods and steps of the metabarcoding procedure.

limited to 26 trees, we still observed strong, statistically supported patterns.

Trees with GOM have fewer fungi and house different fungal communities compared with trees without GOM

Trees with GOM hosted about half of the fungal species hosted by trees without GOM (Figure 2A; Poisson generalized linear model [GLM]; z value = 8.70, $p < 0.001$). The median number of OTUs in trees with GOM was 22, and the median number of OTUs in trees without GOM was 42. Wood with GOM had about 40% of the fungal species richness of wood without GOM (Figure 2C; Poisson GLM; z value = 13.17, $p < 0.001$). The median number of OTUs in wood with GOM was 6, and the median number of OTUs in wood without GOM was 22.

The fungal community compositions of trees with GOM were significantly different from the fungal community compositions of trees without GOM (Figure 2B; adonis; $r^2 = 0.242$, *pseudo-F* = 7.64, $p = 0.0014$), with no significant differences in multivariate dispersion ($p = 0.994$). In wood, differences in fungal community compositions were even more apparent (Figure 2D; adonis; $r^2 = 0.455$, *pseudo-F* = 63.52, $p < 0.001$), and there were significant differences in multivariate dispersion between wood with and without GOM (betadisper; F = 17.491, $p < 0.001$). As validation, we analyzed fungal community compositions after removing the GOM OTU from the community data. Differences between trees and wood with and without GOM remain significant (by tree: adonis; $r^2 = 0.137$, *pseudo-F* = 3.80, $p = 0.034$; by wood: adonis; $r^2 = 0.140$, *pseudo-F* = 11.71, $p < 0.001$).

The most frequently detected fungal OTUs in trees were different when GOM was detected (Table S1). A multivariate GLM revealed 31 fungal OTUs occurred significantly less frequently in trees with GOM. The same analysis revealed 42 fungal OTUs occurred significantly less frequently in wood with GOM. Fungal OTUs in wood with GOM showed decreases in relative prevalence up to 55% compared with wood without GOM (Table S2). By contrast, three fungal OTUs occurred significantly more frequently in wood with GOM: *Armillaria gallica* (FJ744699, SH1057489.09FU), *Blastobotrys farinosus* (OL772661, SH1004482.09FU), and *Hypocreales* sp. (EF619703, SH0978047.09FU).

The ecological guilds of fungal communities also differed in trees and wood with and without GOM. Many of the guilds from trees and wood with GOM had fewer mean guild members

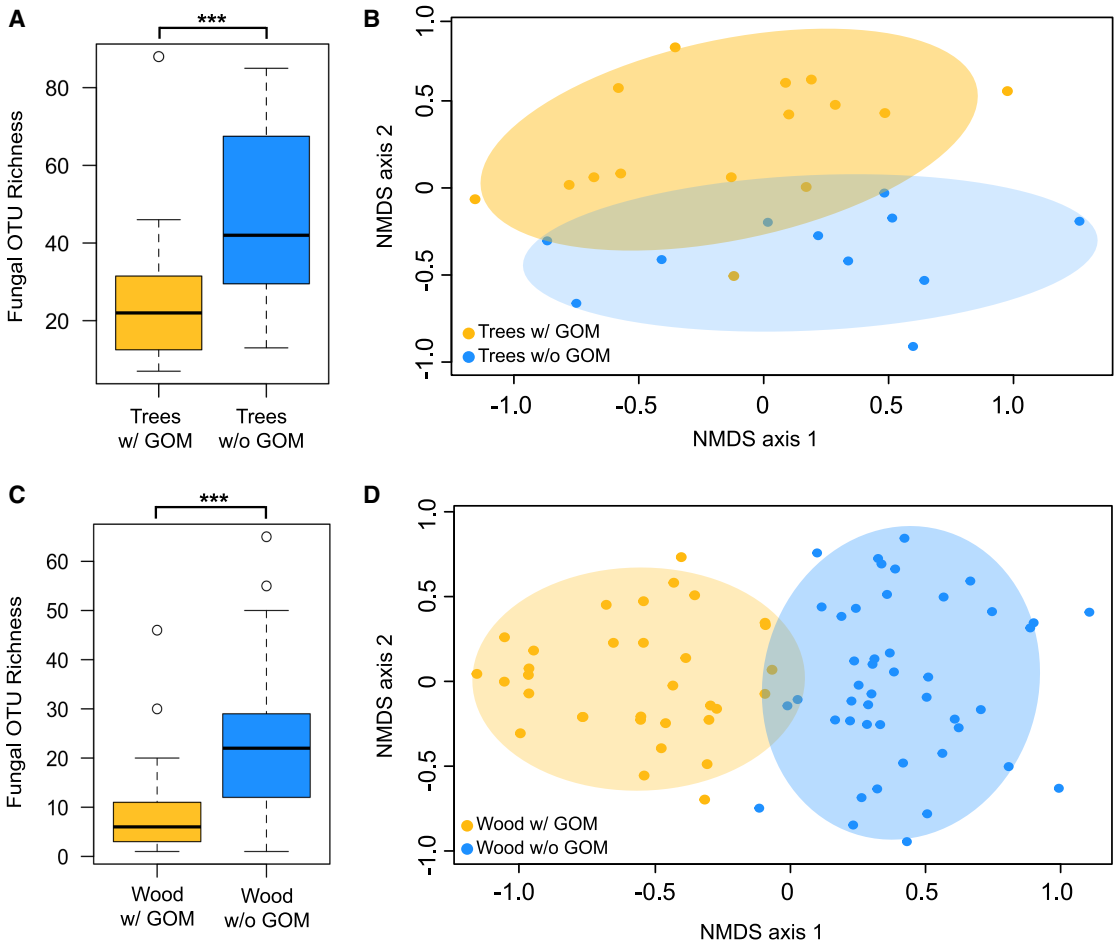

Figure 2. Differences in native fungal richness and community composition in trees and wood with and without GOM

(A) Fungal richness by tree: boxplot of the difference in fungal species richness between trees with and without GOM (using operational taxonomic units [OTUs] as a proxy for species). Trees with GOM had significantly lower fungal species richness than trees without GOM (Poisson GLM; z value = 8.70, $p < 0.001$).

(B) Community composition by tree: NMDS ordination of the difference in fungal communities between trees with and without GOM (stress = 0.120, k = 3), Raup-Crick distance. The fungal communities are significantly different when GOM is present (adonis: $r^2 = 0.242$, *pseudo-F* = 7.64, $p = 0.0014$), with no significant differences in multivariate dispersion (betadisper: $p = 0.994$).

(C) Species richness by wood: boxplot of the difference in fungal species richness between wood sections with and without GOM. Wood with GOM had significantly lower fungal species richness than wood without GOM (Poisson GLM; z value = 13.17, $p < 0.001$).

(D) Community composition by wood: NMDS ordination of the difference in fungal communities between wood sections with and without GOM (stress = 0.140, k = 3), Raup-Crick distance. The fungal communities are significantly different when GOM is present (adonis: $r^2 = 0.455$, *pseudo-F* = 63.522, $p < 0.001$), with significant differences in multivariate dispersion (betadisper; F = 17.491, $p < 0.001$).

For NMDS visualization of communities in wood sections from partially colonized trees, see Figure S1. For ecological guild analyses of these data, see Figure S2. For listing of the most prevalent species in trees with vs. without GOM and species most affected by GOM, see Tables S1 and S2.

than those from trees and wood without GOM, especially the saprotrophic guilds (Figure S2).

GOM has spread quickly and widely

As of December 31, 2023, community science observations recorded GOM in 23 states in the USA and in Ontario, Canada (Figure 3). In the iNaturalist[8] and MushroomObserver[11] databases, the earliest sightings of "escaped" GOM, i.e., uncultivated GOM growing in forests, are single observations in each of the years 2013, 2014, and 2015. In 2013, the fungus was found in Athens, New York; in 2014 in Madison, Wisconsin; and in 2015, at an unspecified location in the state of Ohio (each of these sightings is near the 42nd parallel, between 91°W and 73°W). The total number of North American GOM observations has increased steadily per year since then, with only 5 observations in 2016 building to 2,020 observations in 2023 (Figure 3). Using a convex polygon to estimate range boundaries, the North American range is currently approximately 2 million km^2, as of July 2025. GOM has spread in all directions from the sites where it was originally recorded, and the fungus now spans a range between 29°N and 47°N and 69°W and 105°W in North America.

GOM may spread even further because of climate change

A species distribution model (SDM) developed with curated community science observations and North American climate

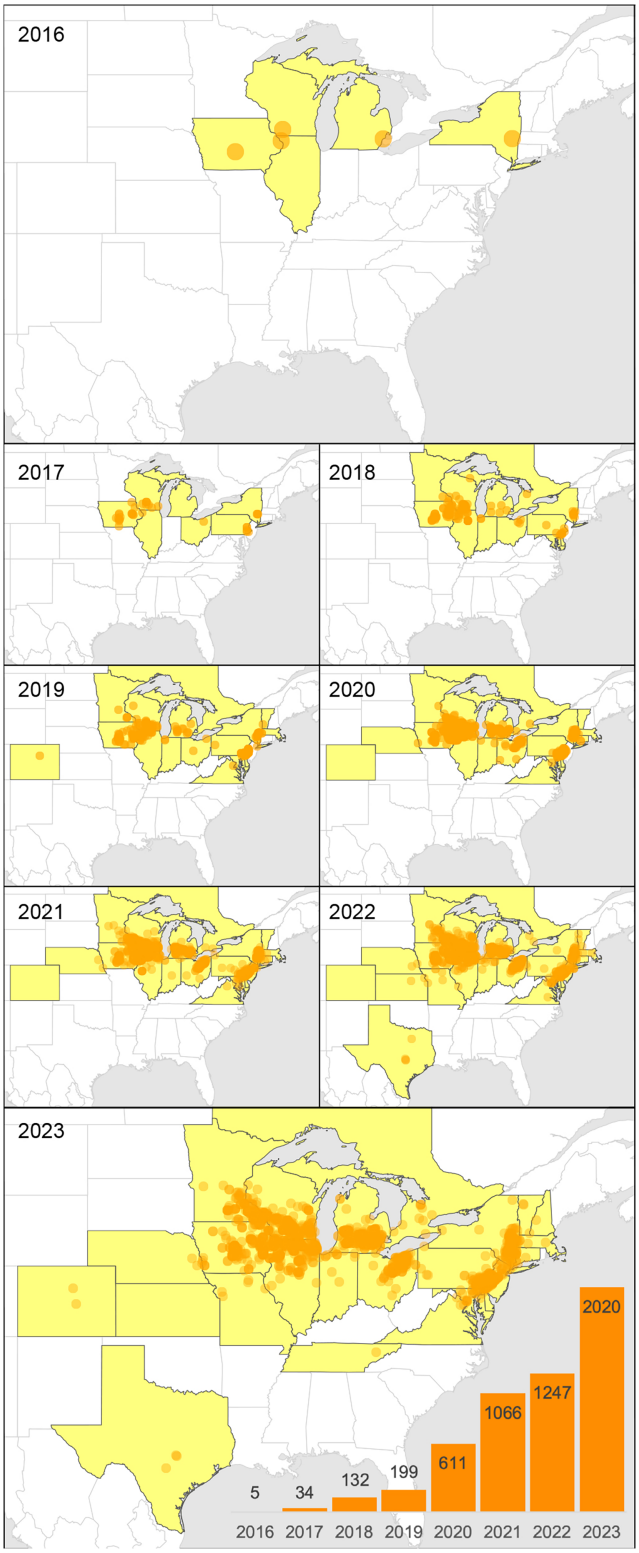

Figure 3. GOM continues to expand its range

Maps of community science observations of GOM per year from iNaturalist and MushroomObserver databases demonstrate the rapid spread of GOM over time. Counts (orange dots) are per year, not cumulative. Color coding of states (yellow = GOM present; white = GOM not present) is cumulative. The bar chart at bottom right shows the increasing number of observations reported each year, non-cumulative. We manually curated each community science observation and excluded observations that were not GOM or were observations of cultivated (not naturalized) GOM. To compare with observations of GOM in its native range, see Figure S3.

data predicts the fungus will be able to expand beyond its current range under the warming climate. Currently uninvaded areas in North America, including the Appalachian Mountain range, the Great Plains region, and Alaska, have at least a 50% probability of being climatically suitable for GOM (Figure 4). Our model performed very well with an area under the receiver operating characteristic (AUC) value of 0.961 with historical climate data and an AUC of 0.919 with simulated future climate data. In our model, the monthly minimum temperature variable had a 79% permutation importance, indicating how heavily the final model depends on this single variable. The monthly precipitation variable had a 21% permutation importance. Per individual tests of variable importance, we found monthly minimum temperature contained the most unique information of all variables, decreased model performance most when omitted, and contained the most useful information on its own.

DISCUSSION

GOM appears to be a strong competitor with dramatic impacts on fungal biodiversity, and our data document a commercially traded mushroom rapidly proliferating and impacting native communities after escaping cultivation and establishing in local forests. Dead trees with GOM house significantly fewer fungal species than dead trees without GOM, and the kinds of fungal communities in trees with or without GOM are very different from each other (Figure 2). We hypothesize the artificial selection of traits desirable to the mushroom cultivation industry, including fast growth, increased temperature tolerance, mold resistance, abundant mushroom production, etc., contributes to the invasive success of GOM.[7,14] Mechanisms mediating the drops in species richness and changes in community composition may include direct interference competition, indirect resource competition,[15] changes in the wood microhabitat and biochemistry mediated by GOM decay,[16–18] or a combination of drivers. If they cannot grow elsewhere, outcompeted fungal individuals (genets) may die,[19] leading to local extinctions of wood-inhabiting species, as well as their unique ecologies and the genetic diversity they carry.[20,21]

Based on our knowledge of fungal biogeography and fungal invasions in Wisconsin, we think the fungal communities we sampled are largely made up of native species; however, we identified one notable exception: *Ophiostoma novo-ulmi*, the non-native causal agent of Dutch Elm disease. The most heavily impacted native species in our survey (Table S2), *Cerrena unicolor*, the "Mossy Maze Polypore," is an efficient fungal producer of therapeutically promising laccase enzymes[22,23] and can have complex symbiotic relationships with woodwasps.[24,25] Another impacted species, *Nemania serpens*, has rich pharmaceutical potential because of its hyper-diverse secondary metabolite gene clusters that differ even between individual isolates.[26] It was 41.4% less prevalent in wood with GOM. Another native GOM-affected fungus in our study, *Hypsizygus ulmarius*,

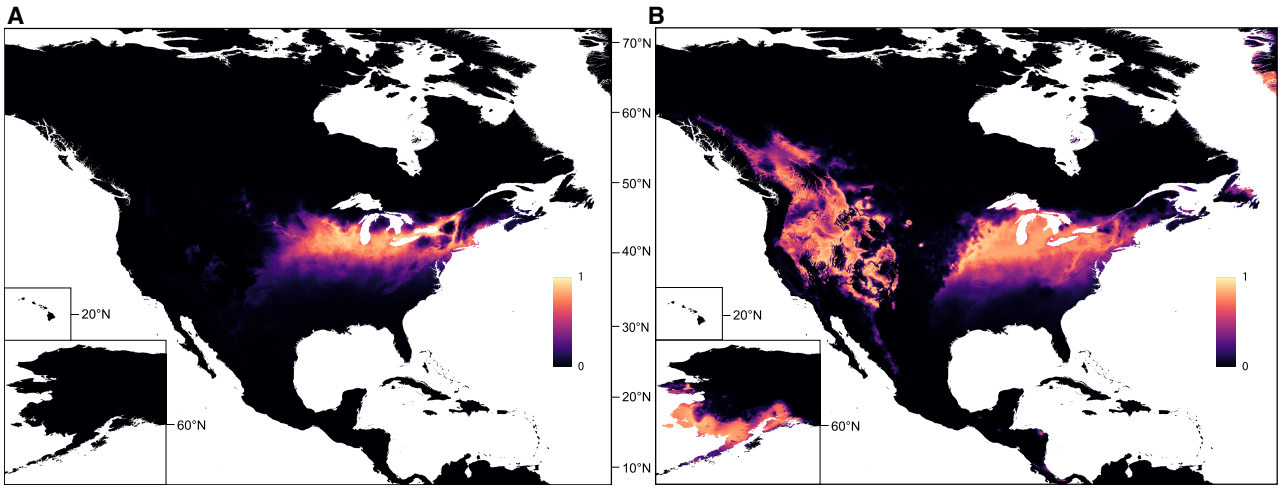

Figure 4. Models of climatically suitable habitat for GOM in North America demonstrating that there are currently uninvaded areas climatically suitable for the fungus

Two SDMs generated by MaxEnt predict where GOM could establish if it is introduced, based on (A) historical climate data and (B) future climate predictions. Both models were trained and tested on the same spatially thinned dataset of observations of GOM from iNaturalist and MushroomObserver and two climate variables: monthly temperature minima and monthly total precipitation. Color scales on the right represent the climatic suitability, with darker colors corresponding to low suitability and brighter colors indicating high suitability.

(A) Model using historical climate data (monthly minimum temperature and precipitation) from 1970–2000. Training AUC = 0.961, test data AUC = 0.961. Jackknife test results of climate variable importance are available in Figure S5.

(B) Model using predicted climate simulations for monthly minimum temperature and precipitation for the years 2021–2040, based on "business as usual/worst case scenario" carbon emissions (Shared Socioeconomic Pathway 5-8.5), simulated by NASA's "GISS-E2-1-G" model.[12,13] Training AUC = 0.925, test data AUC = 0.919. Jackknife test results of climate variable importance are available in Figure S4. For an approximation of GOM's potential biotic niche, see Figure S5.

the "Elm Oyster," is considered monotypic or a single phylospecies,[27] and it represents a distinct pocket of evolutionary diversity. The displacement of these species may be especially consequential because they are biologically unique fungi and singular genetic lineages. However, other fungal species appear to be unaffected by GOM or even to possibly benefit from GOM's presence. For example, *Armillaria gallica* and *Blastobotrys farinosus* are two fungi detected *more* frequently in wood samples with GOM. The guild analysis suggests biodiversity loss is a feature of both the guilds that are common in a dead wood environment, for example, wood saprotrophs, as well as less common guilds, for example, animal parasites and plant pathogens. GOM may also have other, yet undocumented, effects on forest communities and ecosystem processes.

By sampling the same trees at multiple heights, we discovered GOM's effects on fungal communities are localized within the parts of the trees where it is detected, likely reflecting the spatial scales at which wood-inhabiting fungi interact.[20] Seven trees appeared to be only partially colonized, with some heights colonized by GOM and other heights free of GOM. In these wood samples, the fungal communities at heights without GOM resembled the fungal communities in wood from trees completely uninfected by GOM (Figure S1). However, there was no pattern as to which heights were colonized or uncolonized, suggesting GOM is not consistently established at any particular height.

Community science-based observations provide a record of GOM's range expansion and increases in abundance (Figure 3). The proliferation of unique observations of GOM in single areas over time also documents increases in density. GOM has overcome abiotic, biotic, and dispersal barriers to become widespread and dominant. Because GOM is a commercial product and continues to be moved and grown across North America, humans may continue to move it to new areas. In 2019 and 2022, GOM was observed for the first time in Colorado and Texas, respectively, and the observations were made around 800 and 1,000 km from the nearest established GOM population, suggesting human dispersal. Community science observations will continue to be vital for monitoring GOM. Our data (Figure 3) are drawn from observations made through the end of 2023, but as of June 2025, 4,096 new observations have been made in North America, including the first records of GOM in Alabama and Tennessee. Outside of North America, the Global Biodiversity Information Facility (GBIF) database contains observations of GOM growing naturalized in Europe and Africa. While community science databases are subject to bias and unlikely to be complete, the data are often sufficient for estimates of species distributions,[28,29] especially for well-sampled and conspicuous organisms like GOM.

While GOM is currently found in middle and northeastern North America as predicted by the historical climate model, our future climate SDM predicts many more areas in North America are or will become climatically suitable for GOM, for example, forests in the western plains, Appalachia, Alaska, and small parts of Mexico, suggesting GOM will continue to expand its range (Figure 4). The predicted distribution under the current trajectory of climate warming is much greater than the distribution model based on historical climates, highlighting that climate change likely has and will continue to enable GOM's range expansion. Unsurprisingly, GOM's current and predicted ranges share overlap with the latitudes, climate, and mixed hardwood forest

ecosystems of GOM's native range (Figure S3). Both current and predicted distributions of GOM likely correlate with climate and tree species. In our SDM, minimum temperature emerged as a key influence on climatic suitability. Distributions of wood decay fungi correlate with minimum temperature data because fungal metabolism and survival have cold temperature thresholds and because the tree species they decay also have cold-tolerance-related geographic distributions.[16,30] Wood decay fungi have affinities for particular tree species.[31] While the types of wood favored by invasive GOM are not yet fully understood or documented, we observe GOM associating primarily with American elm and note GOM's current distribution is similar to the distribution of American elm. However, GOM has also been reported with black cherry, maple, ash, cottonwoods, mulch, and straw.[8] The native white-rot fungus *Cerioporus squamosus*, the "Dryad's Saddle" or "Pheasant Back" mushroom, often co-occurs with GOM on dead elms, and the current distribution of *C. squamosus* may help predict GOM's potential range (Figure S5). GOM and *C. squamosus* have highly overlapping niches: they are both white-rot fungi, generally grow on hardwood logs, are found in similar climates, and produce mushrooms at similar times of year. Our observation that *C. squamosus* mushrooms were frequently found alongside GOM raises the question of whether these two fungi share any synergistic interactions.

The GOM is aggressively invasive, as suggested by Bruce[7] in their pioneering study documenting the fungus's escape. It is spreading rapidly, increasing in abundance, and disrupting native fungal biodiversity. When the invasive, beetle-cultivated wood decay fungus *Irpex subulatus* was directly inoculated into experimental logs, it also changed fungal community composition,[32] and the similar results across both experimental and natural contexts suggest invasive wood decay fungi may often impact local fungal communities. We present GOM as a literal and figurative bright yellow warning: the globalization of fungi as popular household products can threaten native biodiversity and ecosystem health. In forests where GOM is changing native fungal diversity, it may also be impacting other kinds of forest biodiversity reliant on dead wood, for example, birds, or changing ecosystem dynamics, for example, wood decomposition.[33] As GOM displaces wood-dwelling fungi, it may also affect the biodiversity and interactions of fungal wood decay communities, changing the decay rate of wood and resulting carbon emissions.[34–38] As of now, there are no management strategies available to control its spread.

Global trade directly facilitates non-native species introductions,[39] and the commercialization of fungi has become another opportunity for microbial introductions.[40] Areas where more people buy GOM and then "let it go" into their backyards will have higher propagule pressures, and GOM will be more likely to establish in the areas where it is frequently purchased and grown. Preventing and mitigating the spread of invasive fungi requires addressing the human component of invasions[41–45] by using social impact assessments and communicating with the stakeholders[46,47] using edible fungi, e.g., businesses and consumers. Continued research, management efforts anchored in social theory, and collaborative conversations about microbial endemism can help prevent similar invasions in the future. The cultivation of local species or development of sporeless mushroom strains could also mitigate risks. Conserving fungal biodiversity will be essential to the preservation of the standing genetic variation needed for fungi and forests to adapt to changing environments, particularly in the face of global change.

RESOURCE AVAILABILITY

Lead contact

Further information and requests for resources and reagents should be directed to and will be fulfilled by the lead contact, Aishwarya Veerabahu (veerabahu@wisc.edu).

Materials availability

Fungal cultures used in this study are all available upon request.

Data and code availability

- Fungal community sequence data used to make the figures presented in this work have been deposited at the NCBI Sequence Read Archive and are publicly available as SRA: PRJNA1042626 as of the date of publication.
- All code has been deposited in GitHub and at Zenodo at https://doi.org/10.5281/zenodo.15426686 and is publicly available as of the date of publication.
- Any additional information required to reanalyze the data reported in this paper is available from the lead contact upon request.

ACKNOWLEDGMENTS

We thank the USDA Forest Service Northern Research Station, the University of Wisconsin (UW) Arboretum, the UW-Madison Department of Botany, the Garden Club of America, the Society of Ecological Restoration-Midwest Great Lakes chapter, and the Minnesota Mycological Society for their generous support of this project. We also thank the Madison Parks Department and the UW Arboretum for permission to collect samples. We are grateful to Yu Fukasawa, Zhu-Liang Yang, Yin-Tse Huang, and Che-Chih Chen for records of golden oyster mushrooms from Asia. We deeply thank Sarah Friedrich for assistance with developing figures. We thank Michael Harding for providing guidance with all statistical analyses and James Skelton for assistance with the code. We sincerely appreciate the expertise provided by Carrie Andrew and Benjamin Zuckerberg regarding species distribution modeling. We thank two anonymous reviewers for their thoughtful input that helped improve this manuscript. Thank you to our teams at the Pringle Lab, the USFS NRS Center for Forest Mycology Research, and the Botany Department for all their support. Lastly, we thank every person that posted their observations on iNaturalist and MushroomObserver, discussed this project with us, and shared their ideas and experiences. Our study follows Target 6 of the Kunming-Montreal Biodiversity Framework adopted by the United Nations Biodiversity Conference ("COP15") to analyze and mitigate invasive species' impacts on biodiversity loss.

AUTHOR CONTRIBUTIONS

All authors conceived and designed the study. A.V., A.P., D.L.L., and M.A.J. obtained funding for the project. M.T.B., M.A.J., D.L.L., and A.V. conducted field surveys and obtained necessary permits. M.A.J., M.T.B., and A.V. designed molecular protocols. A.V. and M.A.J. conducted molecular work. A.V. and M.A.J. conducted analysis and bioinformatics. M.A.J., D.L.L., and A.P. contributed resources. A.P. and M.A.J. supervised the project. A.V. wrote the first draft of the manuscript. All authors read and edited the manuscript.

DECLARATION OF INTERESTS

A.P. is vice president of the nonprofit MushroomObserver.

STAR★METHODS

Detailed methods are provided in the online version of this paper and include the following:

- KEY RESOURCES TABLE
- EXPERIMENTAL MODEL AND STUDY PARTICIPANT DETAILS
  - Fungal community survey
- METHOD DETAILS
  - Elm identification
  - Fungal community sequencing
  - Visualization of range expansion
  - Species distribution models
- QUANTIFICATION AND STATISTICAL ANALYSIS
  - Bioinformatics
  - Field survey statistical analyses

SUPPLEMENTAL INFORMATION

Supplemental information can be found online at https://doi.org/10.1016/j.cub.2025.06.049.

Received: December 11, 2024
Revised: March 31, 2025
Accepted: June 18, 2025
Published: July 16, 2025

REFERENCES

1. Pyšek, P., Hulme, P.E., Simberloff, D., Bacher, S., Blackburn, T.M., Carlton, J.T., Dawson, W., Essl, F., Foxcroft, L.C., Genovesi, P., et al. (2020). Scientists' warning on invasive alien species. Biol. Rev. Camb. Philos. Soc. *95*, 1511–1534. https://doi.org/10.1111/brv.12627.
2. Desprez-Loustau, M.L., Robin, C., Buée, M., Courtecuisse, R., Garbaye, J., Suffert, F., Sache, I., and Rizzo, D.M. (2007). The fungal dimension of biological invasions. Trends Ecol. Evol. *22*, 472–480. https://doi.org/10.1016/j.tree.2007.04.005.
3. Gladieux, P., Feurtey, A., Hood, M.E., Snirc, A., Clavel, J., Dutech, C., Roy, M., and Giraud, T. (2015). The population biology of fungal invasions. Mol. Ecol. *24*, 1969–1986. https://doi.org/10.1111/mec.13028.
4. Rizzo, D.M. (2005). Exotic species and fungi: interactions with fungal, plant, and animal communities. In The Fungal Community: Its Organization and Role in the Ecosystem, J. Dighton, J. White, and P. Oudemans, eds. (CRC Press), pp. 857–877. https://doi.org/10.1201/9781420027891.ch43.
5. Singer, R. (1943). Das System der Agaricales. III. Ann. Mycol. *41*, 1–189.
6. Parmasto, E. (1987). Pleurotus citrinopileatus, one of the favourites. Mycologist *1*, 106–107. https://doi.org/10.1016/S0269-915X(87)80076-9.
7. Bruce, A. (2018). Population genomic insights into the establishment of non-native golden oyster mushrooms (Pleurotus citrinopileatus) in the United States. Master's thesis (University of Wisconsin). http://digital.library.wisc.edu/1793/79004.
8. iNaturalist community. (2025). Observations of Pleurotus citrinopileatus from North America observed on/between 01 Jan 2016 - 31 Dec 2023. https://www.inaturalist.org.
9. Blaxter, M., Mann, J., Chapman, T., Thomas, F., Whitton, C., Floyd, R., and Abebe, E. (2005). Defining operational taxonomic units using DNA barcode data. Philos. Trans. R. Soc. Lond. B Biol. Sci. *360*, 1935–1943. https://doi.org/10.1098/rstb.2005.1725.
10. Palmer, J.M., Jusino, M.A., Banik, M.T., and Lindner, D.L. (2018). Non-biological synthetic spike-in controls and the AMPtk software pipeline improve mycobiome data. PeerJ *6*, e4925. https://doi.org/10.7717/peerj.4925.
11. Mushroom Observer. (2025). Observations of Pleurotus citrinopileatus from North America observed on/between 01 Jan 2016 - 31 Dec 2023. https://mushroomobserver.org/.
12. NASA Goddard Institute for Space Studies (NASA/GISS) (2018). NASA-GISS GISS-E2.1G model output prepared for CMIP6 CMIP. Version 20230720 (Earth System Grid Federation). https://doi.org/10.22033/ESGF/CMIP6.1400.
13. Eyring, V., Bony, S., Meehl, G.A., Senior, C.A., Stevens, B., Stouffer, R.J., and Taylor, K.E. (2016). Overview of the Coupled Model Intercomparison Project Phase 6 (CMIP6) experimental design and organization. Geosci. Model Dev. *9*, 1937–1958. https://doi.org/10.5194/gmd-9-1937-2016.
14. Barh, A., Sharma, V.P., Annepu, S.K., Kamal, S., Sharma, S., and Bhatt, P. (2019). Genetic improvement in Pleurotus (oyster mushroom): a review. 3 Biotech *9*, 322. https://doi.org/10.1007/s13205-019-1854-x.
15. Begon, M., Harper, J.L., and Townsend, C.R. (1996). Interspecific Competition. In Ecology: Individuals, Populations, and Communities (Wiley-Blackwell), pp. 265–312.
16. Heilmann-Clausen, J., and Boddy, L. (2008). Distribution patterns of wood-decay basidiomycetes at the landscape to global scale. In Ecology of Saprotrophic Basidiomycetes British Mycological Society Symposia Series (Elsevier), pp. 263–275. https://doi.org/10.1016/S0275-0287(08)80016-1.
17. Woodward, S., and Boddy, L. (2008). Interactions between saprotrophic fungi. In British Mycological Society Symposia Series (Elsevier), pp. 125–141. https://doi.org/10.1016/S0275-0287(08)80009-4.
18. Hiscox, J., Savoury, M., Johnston, S.R., Parfitt, D., Müller, C.T., Rogers, H.J., and Boddy, L. (2016). Location, location, location: priority effects in wood decay communities may vary between sites. Environ. Microbiol. *18*, 1954–1969. https://doi.org/10.1111/1462-2920.13141.
19. Boddy, L., and Hiscox, J. (2016). Fungal Ecology: Principles and Mechanisms of Colonization and Competition by Saprotrophic Fungi. Microbiol. Spectr. *4*. https://doi.org/10.1128/microbiolspec.FUNK-0019-2016.
20. Boddy, L. (2000). Interspecific combative interactions between wood-decaying basidiomycetes. FEMS Microbiol. Ecol. *31*, 185–194. https://doi.org/10.1111/j.1574-6941.2000.tb00683.x.
21. Moor, H., Nordén, J., Penttilä, R., Siitonen, J., and Snäll, T. (2021). Long-term effects of colonization–extinction dynamics of generalist versus specialist wood-decaying fungi. J. Ecol. *109*, 491–503. https://doi.org/10.1111/1365-2745.13526.
22. Matuszewska, A., Karp, M., Jaszek, M., Janusz, G., Osińska-Jaroszuk, M., Sulej, J., Stefaniuk, D., Tomczak, W., and Giannopoulos, K. (2016). Laccase purified from Cerrena unicolor exerts antitumor activity against leukemic cells. Oncol. Lett. *11*, 2009–2018. https://doi.org/10.3892/ol.2016.4220.
23. Janusz, G., Rogalski, J., and Szczodrak, J. (2007). Increased production of laccase by Cerrena unicolor in submerged liquid cultures. World J. Microbiol. Biotechnol. *23*, 1459–1464. https://doi.org/10.1007/s11274-007-9390-y.
24. Kuramitsu, K., Kosaki, A., Ishihara, T., Yamada, H., and Watanabe, K. (2016). Infestation of the woodwasp *Tremex apicalis* Matsumura (Hymenoptera, Siricidae) on the large-leaf dogwood *Swida macrophylla* (Wall.) with biological notes on its parasitoid wasps. J. Hymenopt. Res. *52*, 71–79. https://doi.org/10.3897/jhr.52.10060.
25. Pažoutová, S., and Šrůtka, P. (2007). Symbiotic relationship between *Cerrena unicolor* and the horntail *Tremex fuscicornis* recorded in the Czech Republic. Czech Mycol. *59*, 83–90. https://doi.org/10.33585/cmy.59109.
26. Franco, M.E.E., Wisecaver, J.H., Arnold, A.E., Ju, Y.M., Slot, J.C., Ahrendt, S., Moore, L.P., Eastman, K.E., Scott, K., Konkel, Z., et al. (2022). Ecological generalism drives hyperdiversity of secondary metabolite gene clusters in Xylarialean endophytes. New Phytol. *233*, 1317–1330. https://doi.org/10.1111/nph.17873.
27. Bellanger, J.M., Moreau, P.A., Corriol, G., Bidaud, A., Chalange, R., Dudova, Z., and Richard, F. (2015). Plunging hands into the mushroom jar: a

phylogenetic framework for Lyophyllaceae (Agaricales, Basidiomycota). Genetica *143*, 169–194. https://doi.org/10.1007/s10709-015-9823-8.

28. Johnston, A., Moran, N., Musgrove, A., Fink, D., and Baillie, S.R. (2020). Estimating species distributions from spatially biased citizen science data. Ecol. Modell. *422*, 108927. https://doi.org/10.1016/j.ecolmodel.2019.108927.
29. Robinson, O.J., Ruiz-Gutierrez, V., Reynolds, M.D., Golet, G.H., Strimas-Mackey, M., and Fink, D. (2020). Integrating citizen science data with expert surveys increases accuracy and spatial extent of species distribution models. Divers. Distrib. *26*, 976–986. https://doi.org/10.1111/ddi.13068.
30. Venugopal, P., Junninen, K., Linnakoski, R., Edman, M., and Kouki, J. (2016). Climate and wood quality have decayer-specific effects on fungal wood decomposition. For. Ecol. Manag. *360*, 341–351. https://doi.org/10.1016/j.foreco.2015.10.023.
31. Rustøen, F., Høiland, K., Heegaard, E., Boddy, L., Gange, A.C., Kauserud, H., and Andrew, C. (2023). Substrate affinities of wood decay fungi are foremost structured by wood properties not climate. Fungal Ecol. *63*, 101231. https://doi.org/10.1016/j.funeco.2023.101231.
32. Jusino, M.A., Skelton, J., Chen, C.-C., Hulcr, J., and Smith, M.E. (2020). Sexual reproduction and saprotrophic dominance by the ambrosial fungus *Flavodon subulatus* (= *Flavodon ambrosius*). Fungal Ecol. *47*, 100979. https://doi.org/10.1016/j.funeco.2020.100979.
33. Fukasawa, Y. (2021). Ecological impacts of fungal wood decay types: A review of current knowledge and future research directions. Ecol. Res. *36*, 910–931. https://doi.org/10.1111/1440-1703.12260.
34. Rayner, A.D.M., and Boddy, L. (1988). Fungal communities in the decay of wood. In Advances in Microbial Ecology Advances in Microbial Ecology, K.C. Marshall, ed. (Springer), pp. 115–166. https://doi.org/10.1007/978-1-4684-5409-3_4.
35. Lustenhouwer, N., Maynard, D.S., Bradford, M.A., Lindner, D.L., Oberle, B., Zanne, A.E., and Crowther, T.W. (2020). A trait-based understanding of wood decomposition by fungi. Proc. Natl. Acad. Sci. USA *117*, 11551–11558. https://doi.org/10.1073/pnas.1909166117.
36. Maynard, D.S., Bradford, M.A., Covey, K.R., Lindner, D., Glaeser, J., Talbert, D.A., Tinker, P.J., Walker, D.M., and Crowther, T.W. (2019). Consistent trade-offs in fungal trait expression across broad spatial scales. Nat. Microbiol. *4*, 846–853. https://doi.org/10.1038/s41564-019-0361-5.
37. Yang, C., Schaefer, D.A., Liu, W., Popescu, V.D., Yang, C., Wang, X., Wu, C., and Yu, D.W. (2016). Higher fungal diversity is correlated with lower CO2 emissions from dead wood in a natural forest. Sci. Rep. *6*, 31066. https://doi.org/10.1038/srep31066.
38. Bradford, M.A., Maynard, D.S., Crowther, T.W., Frankson, P.T., Mohan, J.E., Steinrueck, C., Veen, G.F.C., King, J.R., and Warren, R.J. (2021). Belowground community turnover accelerates the decomposition of standing dead wood. Ecology *102*, e03484. https://doi.org/10.1002/ecy.3484.
39. Blackburn, T.M., Pyšek, P., Bacher, S., Carlton, J.T., Duncan, R.P., Jarošík, V., Wilson, J.R.U., and Richardson, D.M. (2011). A proposed unified framework for biological invasions. Trends Ecol. Evol. *26*, 333–339. https://doi.org/10.1016/j.tree.2011.03.023.
40. Desprez-Loustau, M.-L. (2009). Alien fungi of Europe. In Handbook of Alien Species in Europe (Springer Netherlands), pp. 15–28. https://doi.org/10.1007/978-1-4020-8280-1_2.
41. Dickie, I.A., Nuñez, M.A., Pringle, A., Lebel, T., Tourtellot, S.G., and Johnston, P.R. (2016). Towards management of invasive ectomycorrhizal fungi. Biol. Invasions *18*, 3383–3395. https://doi.org/10.1007/s10530-016-1243-x.
42. Schwartz, M.W., Hoeksema, J.D., Gehring, C.A., Johnson, N.C., Klironomos, J.N., Abbott, L.K., and Pringle, A. (2006). The promise and the potential consequences of the global transport of mycorrhizal fungal inoculum. Ecol. Lett. *9*, 501–515. https://doi.org/10.1111/j.1461-0248.2006.00910.x.
43. Larson, D.L., Phillips-Mao, L., Quiram, G., Sharpe, L., Stark, R., Sugita, S., and Weiler, A. (2011). A framework for sustainable invasive species management: Environmental, social, and economic objectives. J. Environ. Manage. *92*, 14–22. https://doi.org/10.1016/j.jenvman.2010.08.025.
44. Novoa, A., Dehnen-Schmutz, K., Fried, J., and Vimercati, G. (2017). Does public awareness increase support for invasive species management? Promising evidence across taxa and landscape types. Biol. Invasions *19*, 3691–3705. https://doi.org/10.1007/s10530-017-1592-0.
45. Shapiro, H.G., Willcox, A.S., Willcox, E.V., and Verant, M.L. (2022). U.S. National Park visitor perceptions and behavioral intentions towards actions to prevent white-nose syndrome. PLoS One *17*, e0278024. https://doi.org/10.1371/journal.pone.0278024.
46. Estévez, R.A., Anderson, C.B., Pizarro, J.C., and Burgman, M.A. (2015). Clarifying values, risk perceptions, and attitudes to resolve or avoid social conflicts in invasive species management. Conserv. Biol. *29*, 19–30. https://doi.org/10.1111/cobi.12359.
47. Crowley, S.L., Hinchliffe, S., and McDonald, R.A. (2017). Invasive species management will benefit from social impact assessment. J. Appl. Ecol. *54*, 351–357. https://doi.org/10.1111/1365-2664.12817.
48. Lindner, D.L., and Banik, M.T. (2009). Effects of cloning and root-tip size on observations of fungal ITS sequences from *Picea glauca* roots. Mycologia *101*, 157–165. https://doi.org/10.3852/08-034.
49. Taberlet, P., Gielly, L., Pautou, G., and Bouvet, J. (1991). Universal primers for amplification of three non-coding regions of chloroplast DNA. Plant Mol. Biol. *17*, 1105–1109. https://doi.org/10.1007/BF00037152.
50. Ihrmark, K., Bödeker, I.T.M., Cruz-Martinez, K., Friberg, H., Kubartova, A., Schenck, J., Strid, Y., Stenlid, J., Brandström-Durling, M., Clemmensen, K.E., et al. (2012). New primers to amplify the fungal ITS2 region - evaluation by 454-sequencing of artificial and natural communities. FEMS Microbiol. Ecol. *82*, 666–677. https://doi.org/10.1111/j.1574-6941.2012.01437.x.
51. R Core Team (2024). R: A Language and Environment for Statistical Computing (R Foundation for Statistical Computing). https://www.R-project.org.
52. Phillips, S.J., Anderson, R.P., and Schapire, R.E. (2006). Maximum entropy modeling of species geographic distributions. Ecol. Model. *190*, 231–259. https://doi.org/10.1016/j.ecolmodel.2005.03.026.
53. Nguyen, N.H., Song, Z., Bates, S.T., Branco, S., Tedersoo, L., Menke, J., Schilling, J.S., and Kennedy, P.G. (2016). FUNGuild: An open annotation tool for parsing fungal community datasets by ecological guild. Fungal Ecol. *20*, 241–248. https://doi.org/10.1016/j.funeco.2015.06.006.
54. Hijmans, R.J., Cameron, S.E., Parra, J.L., Jones, P.G., and Jarvis, A. (2005). Very high resolution interpolated climate surfaces for global land areas. Int. J. Climatol. *25*, 1965–1978. https://doi.org/10.1002/joc.1276.
55. Gilmartin, E.C., Jusino, M.A., Pyne, E.J., Banik, M.T., Lindner, D.L., and Boddy, L. (2022). Fungal endophytes and origins of decay in beech (*Fagus sylvatica*) sapwood. Fungal Ecol. *59*, 101161. https://doi.org/10.1016/j.funeco.2022.101161.
56. Jusino, M.A., Lindner, D.L., Cianchetti, J.K., Grisé, A.T., Brazee, N.J., and Walters, J.R. (2014). A minimally invasive method for sampling nest and roost cavities for fungi: a novel approach to identify the fungi associated with cavity-nesting birds. Acta Ornithol. *49*, 233–242. https://doi.org/10.3161/173484714X687127.
57. White, T.J., Bruns, T., Lee, S., and Taylor, J. (1990). Amplification and direct sequencing of fungal ribosomal RNA genes for phylogenetics. In PCR Protocols: A Guide to Methods and Applications (Academic Press), pp. 315–322. https://doi.org/10.1016/B978-0-12-372180-8.50042-1.
58. Gardes, M., and Bruns, T.D. (1993). ITS primers with enhanced specificity for basidiomycetes – application to the identification of mycorrhizae and rusts. Mol. Ecol. *2*, 113–118. https://doi.org/10.1111/j.1365-294X.1993.tb00005.x.
59. Massicotte, P., and South, A. (2023). rnaturalearth: World Map Data from Natural Earth. R package version 1.0.1. https://CRAN.R-project.org/package=rnaturalearth.

60. Wickham, H. (2016). ggplot2 (Springer International Publishing). https://doi.org/10.1007/978-3-319-24277-4.

61. Pebesma, E. (2018). Simple Features for R: Standardized Support for Spatial Vector Data. R J. *10*, 439. https://doi.org/10.32614/RJ-2018-009.

62. Google Earth. (2021). GOM - Current Invasive Range in North America. 2D Polygon feature. https://earth.google.com/earth/d/1R4ueNi5qqGHUZBdWnOn3VvaUg7lxhQRP?usp=sharing.

63. Wollan, A.K., Bakkestuen, V., Kauserud, H., Gulden, G., and Halvorsen, R. (2008). Modelling and predicting fungal distribution patterns using herbarium data. J. Biogeogr. *35*, 2298–2310. https://doi.org/10.1111/j.1365-2699.2008.01965.x.

64. Elith, J., Graham, H., Dudík, M., Ferrier, S., Guisan, A., Dudík, M., Huettmann, F., Guisan, A., Lehmann, A., et al. (2006). Novel methods improve prediction of species' distributions from occurrence data. Ecography *29*, 129–151. https://doi.org/10.1111/j.2006.0906-7590.04596.x.

65. Aiello-Lammens, M.E., Boria, R.A., Radosavljevic, A., Vilela, B., and Anderson, R.P. (2015). spThin: an R package for spatial thinning of species occurrence records for use in ecological niche models. Ecography *38*, 541–545. https://doi.org/10.1111/ecog.01132.

66. Phillips, S.J., and Dudík, M. (2008). Modeling of species distributions with Maxent: new extensions and a comprehensive evaluation. Ecography *31*, 161–175. https://doi.org/10.1111/j.0906-7590.2008.5203.x.

67. Barbet-Massin, M., Jiguet, F., Albert, C.H., and Thuiller, W. (2012). Selecting pseudo-absences for species distribution models: how, where and how many? Methods Ecol. Evol. *3*, 327–338. https://doi.org/10.1111/j.2041-210X.2011.00172.x.

68. Peterson, A.T., Soberón, J., Pearson, R.G., Anderson, R.P., Martínez-Meyer, E., Nakamura, M., and Araújo, M.B. (2011). Evaluating model performance and significance. In Ecological Niches and Geographic Distributions (Princeton University Press), pp. 150–184. https://doi.org/10.23943/princeton/9780691136868.003.0009.

69. Edgar, R.C. (2016). UNOISE2: improved error-correction for Illumina 16S and ITS amplicon sequencing. Preprint at bioRxiv. https://doi.org/10.1101/081257.

70. Abarenkov, K., Nilsson, R.H., Larsson, K.-H., Taylor, A.F.S., May, T.W., Frøslev, T.G., Pawlowska, J., Lindahl, B., Põldmaa, K., Truong, C., et al. (2024). The UNITE database for molecular identification and taxonomic communication of fungi and other eukaryotes: sequences, taxa and classifications reconsidered. Nucleic Acids Res. *52*, D791–D797. https://doi.org/10.1093/nar/gkad1039.

71. Oksanen, J., Simpson, G.L., Blanchet, F.G., Kindt, R., Legendre, P., Minchin, P.R., O'Hara, R.B., Solymos, P., Stevens, M.H.H., Szoecs, E., et al. (2022). vegan: Community Ecology Package. R package version 2.6-8. https://CRAN.R-project.org/package=vegan.

72. Wang, Y., Naumann, U., Wright, S.T., and Warton, D.I. (2012). mvabund–an R package for model-based analysis of multivariate abundance data. Methods Ecol. Evol. *3*, 471–474. https://doi.org/10.1111/j.2041-210X.2012.00190.x.

73. Chase, J.M., Kraft, N.J.B., Smith, K.G., Vellend, M., and Inouye, B.D. (2011). Using null models to disentangle variation in community dissimilarity from variation in α-diversity. Ecosphere *2*, 24. https://doi.org/10.1890/ES10-00117.1.

74. Anderson, M.J. (2001). A new method for non-parametric multivariate analysis of variance. Austral Ecol. *26*, 32–46. https://doi.org/10.1111/j.1442-9993.2001.01070.pp.x.

75. Anderson, M.J., Ellingsen, K.E., and McArdle, B.H. (2006). Multivariate dispersion as a measure of beta diversity. Ecol. Lett. *9*, 683–693. https://doi.org/10.1111/j.1461-0248.2006.00926.x.

STAR★METHODS

KEY RESOURCES TABLE

REAGENT or RESOURCE	SOURCE	IDENTIFIER
Biological samples		
Drilled wood from 26 dead *Ulmus* trees	this paper	N/A
Basidiocarps of *Pleurotus citrinopileatus*	this paper	N/A
Basidiocarps of *Pleurotus pulmonarius*	this paper	N/A
Basidiocarps of *Trametes versicolor*	this paper	N/A
Chemicals, peptides, and recombinant proteins		
CLS/CTAB Lysis Buffer	Lindner and Banik[48]	N/A
Critical commercial assays		
GeneClean III Kit	MP Biomedicals	SKU 111001601
Deposited data		
Illumina reads from drilled wood samples (raw and analyzed data)	This paper	PRJNA1042626
Oligonucleotides		
Synthetic Mock Community control	Palmer et al.[10]	N/A
Primers for *trnL* gene; trnL_c (forward): CGAAATCGGTAGACGCTACG; trnL_d (reverse): GGGGATAGAGGGACTTGAAC	Taberlet et al.[49]	N/A
Primers for ITS region; ITS1F (forward): CTTGGTCATTTAGAGGAAGTAA; ITS7 (forward): GTGARTCATCGARTCTTTG; ITS4 (reverse): TCCTCCGCTTATTGATATGC	Ihrmark et al.[50]	N/A
Software and algorithms		
R Studio Version 4.2.2	R Core Team[51]	https://www.r-project.org
AMPtk v1.6.0	Palmer et al.[10]	https://amptk.readthedocs.io/en/latest/
MaxEnt	Phillips et al.[52]	https://biodiversityinformatics.amnh.org/open_source/maxent/
Geneious Prime v2023.1.2	Geneious	https://www.geneious.com/
FUNGuild v2.0	Nguyen et al. 2016[53]	http://www.funguild.org
Code	This paper	https://github.com/AishwaryaV7/GOM-2024.git
Other		
Pleurotus citronpileatus public occurrence data	iNaturalist[8]	https://www.inaturalist.org/observations?place_id=97394&subview=map&taxon_id=504060
Pleurotus citronpileatus public occurrence data	Mushroom Observer[11]	https://mushroomobserver.org/?advanced_search=1&q=1pOzE
WorldClim climate data	Hijmans et al.[54]	https://worldclim.org/data/worldclim21.html

EXPERIMENTAL MODEL AND STUDY PARTICIPANT DETAILS

Fungal community survey

We surveyed the University of Wisconsin-Madison Arboretum, Owen Conservation Park, and Quarry Park in Madison, Wisconsin, United States for dead elms with and without golden oyster mushroom (GOM; *Pleurotus citrinopileatus* Singer [Agaricales, Basidiomycota]) basidiocarps using a paired sample design. For each tree with GOM we identified, we located a dead elm (*Ulmus* sp.) lacking evidence of GOM colonization, found in proximity (within a 50 m radius) and of similar decay stage. A total of 13 such pairs (26 trees) were sampled for fungal community analysis using metabarcoding over the three sites. Wood shavings from these trees were collected by using a hatchet to reveal a clean section of interior wood and drilling a total of nine 0.8 cm diameter holes approximately 10 cm deep, using an electric battery-operated drill, DNA-sterile drill bits, and DNA-sterile funnels for each height per tree to collect the wood shavings.[55] Three drillings, spaced evenly about the trunk circumference, were taken from each of three heights: 0.3 m, 1.5 m, and 2.7 m (1 ft, 5 ft, and 9 ft) from the base of the tree to capture potential differences in the fungal community at different

heights and maximize the probability of detecting GOM (Figure 1). Samples from different heights were kept separate to inform future sampling efforts (see "tree" and "wood" definitions in field survey statistical analyses section) resulting in 78 samples. At the end of each day of field collection, DNA-sterile cell lysis solution[48] (CLS) was added to all samples in a sterile hood to completely submerge the shavings. Samples were stored at -20°C until prepped for extraction. Control samples included negative field controls for each tree and lab negative controls for each sampling day.

METHOD DETAILS

Elm identification

To confirm the identity of the dead trees sampled as elms (*Ulmus*), we used a combination of DNA identification and morphological identification when DNA identification was not possible. Genomic DNA was extracted from wood shaving samples using a modified version of the GeneClean III Kit (MP Biomedicals, Santa Ana, CA) protocol, following the methods of Lindner and Banik and Jusino et al.[48,56] The *trnL* region of the chloroplast tRNA gene was amplified using trn*L-c* and trn*L-d*.[49] PCR amplification used the following reagent volumes and concentrations per 15 μL reaction: 7.88 μL DNA-free molecular grade water, 3 μL Green GoTaq 5x buffer (Promega Corporation, Madison, WI, USA)—final concentration 1x, 0.12 μL of 20 mg/mL BSA (New England BioLabs, Ipswich, MA), 0.3 μL of 10 mM dNTPs (Promega Corporation, Madison, WI, USA)—final concentration 200 μM of each dNTP, 0.3 μL of each 10 μM primer—final concentration of 0.2 μM of each primer, 0.1 μL of 5uM GoTaq polymerase (Promega Corporation, Madison, WI, USA)—final concentration of 0.033uM, and 3 μL of extracted template DNA. Thermal cycler parameters were as follows: 95°C for 3 minutes, then 35 cycles of (95°C for 30 s, 53°C for 60 s, 72°C for 60 s), followed by 72°C for 5 min), then kept at an 8°C hold. PCR products were gel visualized to confirm amplification. Amplified products were diluted and combined with Sanger sequencing reagents from the QuantumDye v3.1 kit (SureFire Biosciences, San Diego, CA, USA) using the following reagent volumes: 1.8 μL DNA-free molecular grade water, 2.5 μL 5x QuantumDye sequencing buffer—final concentration 1x, 0.5 μL 5M betaine (Sigma-Aldrich, St. Louis, MO, USA) —final concentration 0.2 μM, 0.5 μL 2.5x QuantumDye cycle sequencing mix—final concentration 0.1x, 0.2 μL of each 10 μM primer—final concentration of 0.16 μM of each primer, and 7 μL of diluted PCR product. Products were terminally amplified in a Sanger PCR reaction under the following conditions: 96°C for 30 s (ramp 1°/s), 50°C for 30 s (ramp 1°/s), 60°C for 3 minutes (ramp 1°/s), for 31 cycles, then kept at a 4°C hold. Samples were submitted for sequencing at Functional Biosciences, Madison, WI, USA. Sequences were analyzed using Geneious (Dotmatics Corporation, Boston, MA, USA) and checked against the NCBI database for identification. For morphological identification of the genus and species of sampled trees, we looked at unique identifying features including bark color, bark pattern, the layered pattern and coloration of bark cross sections, buttressing roots, and similarity to trees we molecularly confirmed to be elm. The trees sampled were all confirmed to be elms (*Ulmus* sp.), *Ulmus americana* (24 of 26 trees) and *Ulmus rubra* (2 trees), by either DNA-based identification (20 of 26 trees) or morphological identification (6 trees).

Fungal community sequencing

The fungal community composition of each dead elm with and without GOM was measured using metabarcoding techniques. Samples were prepared for DNA extraction by incubating for 2 hours in a 65°C water bath. Genomic DNA was extracted from wood shaving samples using a modified version of the GeneClean III Kit (MP Biomedicals, Santa Ana, CA) protocol, following the methods of Lindner and Banik and Jusino et al.[48,56]

The partial internal transcribed spacer region (ITS2) was amplified using ITS-7[50] and ITS-4[57] primers modified with Illumina Nextera v2 adapters (Illumina, San Diego, CA, USA). Initial PCR amplification of the ITS2 region used the following reagent volumes and concentrations per 15 μL reaction: 7.88 μL DNA-free molecular grade water, 3 μL Green GoTaq 5x buffer (Promega Corporation, Madison, WI, USA)—final concentration 1x; 0.12 μL of 20 mg/mL BSA (New England BioLabs, Ipswich, MA), 0.3 μL of 10 mM dNTPs (Promega Corporation, Madison, WI, USA)—final concentration 200 μM of each dNTP; 0.3 μL of each 10 μM primer—final concentration of 0.2 μM of each primer; 0.1 μL of 5uM GoTaq polymerase (Promega Corporation, Madison, WI, USA)—final concentration of 0.033u/μL of the reaction; and 3 μL of extracted template DNA. The initial PCR used the following amplification conditions: 94°C for 3 minutes, then 11 cycles of (94°C for 30 s, 60°C for 30 s, decreasing by 0.5°C / cycle, then 72°C for 1 min), followed by 26 cycles of (94°C for 30 s, 55°C for 30 s, and 72°C for 1 min), then held at 8°C. PCR products were gel visualized to confirm amplification. After initial amplification, samples were dual-indexed by PCR using Illumina Nextera v2 indices (Illumina Inc., San Diego, CA, USA), and the following reagent volumes and concentrations: 16.13 μL DNA-free molecular grade water; 5 μL Green GoTaq 5x buffer (Promega Corporation, Madison, WI, USA)—final concentration 1x; 0.5 μL of 10 mM dNTPs (Promega Corporation, Madison, WI, USA)—final concentration 200 μM of each dNTP; 0.5 μL of each 10 μL primer—final concentration of 0.2 μM of each index primer; 0.2 μL of 20 mg/mL BSA (New England BioLabs, Ipswich, MA); 0.17 μL of 5uM GoTaq polymerase (Promega Corporation, Madison, WI, USA)—final concentration of 0.033 μM; and 2 μL of products from the initial PCR. The second amplification used the following conditions: 94°C for 2 min, followed by 8 cycles of (94°C for 30 s, 53°C for 30 s, then 72°C for 1 min), then 72°C for 5 min. Negative controls were included for each PCR step. Indexed products were then cleaned using Zymo Select-A-Size DNA Clean and Concentrator spin columns (Zymo Research, Irvine, CA, 264 USA, quantified DNA), quantified using a Qubit Flex Fluorometer and high sensitivity dsDNA Assay (ThermoFisher Scientific, Madison, WI, USA), and pooled in equal concentrations for Illumina MiSeq (2 x 300bp) v3 sequencing at the University of California Riverside Genomics Core Center.

In addition to the extracted wood samples and negative controls, a question-specific biological community control ("biomock") and a single-copy synthetic mock community control[10] (SynMock) were also amplified and sequenced. In addition to helping parameterize clustering, SynMock helps to reduce the bioinformatic errors caused by tag-switching in multiplexed samples in metabarcoding. Biomock serves as a question-specific positive control containing known specimens that may be found in the community data, in this instance: *Pleurotus citrinopileatus*, *Pleurotus ostreatus*, and *Trametes versicolor*. Specimens were collected from forests around southern Wisconsin and are part of the Center for Forest Mycology Research (CFMR) culture collection. DNA of pure cultures of each species listed were extracted as described above and Sanger sequenced to confirm identity using unmodified ITS1F[58] and ITS4 primers to amplify the ITS region. The PCR conditions used the same reagent volumes and concentrations as described above and the thermal cycler profile was as follows: 94°C for 3 min, followed by 31 cycles of (94°C for 60 s, 53°C for 60 s, then 72°C for 3 min), then 72°C for 10 min. Samples were combined with Sanger sequencing reagents and terminally amplified as described above. Samples were submitted for sequencing at Functional Biosciences, Madison, WI, USA. Sequences were analyzed using Geneious v2023.1.2 (Dotmatics Corporation, Boston, MA, USA) and checked against the NCBI database for identification. DNA of these samples was quantified and pooled in equal concentrations. SynMock's composition is described in detail in Palmer et al.[10] Both biomock and SynMock were amplified, indexed, cleaned, quantified, and pooled with all samples as described above.

Visualization of range expansion

To document the expansion of GOM's current distribution, we used occurrence records identified as *Pleurotus citrinopileatus* Singer from 2016 - 2023, downloaded from iNaturalist.com and MushroomObserver.com, the two major databases used in North America for fungal observations, on January 2nd, 2024. The records from iNaturalist and MushroomObserver were curated based on visual evidence of naturalization on coarse-size deadwood, excluding occurrences that were deemed to be cultivated or growing on mulch in a garden-bed or similar set-up. The remaining occurrences were used to create current range maps of GOM's occurrence and spread over the last eight years using R[51] with the packages rnaturalearth,[59] ggplot2,[60] and sf.[61] To estimate the size of GOM's current range, we used the "Measure" tool in Google Earth v10.64.0.3[62] which calculates the square area of a user-defined convex polygon overlaid on North America, which we bounded to include the locations of the outermost observations of GOM.

Species distribution models

To estimate the potential expansion of GOM's range, we developed a predictive species distribution model (SDM) based on the observed climatic niche of current occurrences of GOM in North America combined with climate data from the past 50 years. We used the program MAXENT version 3.4.4[52] as it has been successfully used to model the distribution of macrofungi[63] and shown to perform better than some other SDM algorithms when presence-only data are used in conjunction with background data.[64] Maxent is also capable of producing accurate models based on spatially-biased, nonrandom occurrence data by sampling background points or using pseudo-absence data.

We used curated (see above) North American observations of GOM prior to 2024 from iNaturalist and Mushroom Observer to accurately capture the niche of the naturalized North American strains and train and test our model. Occurrence data was spatially thinned to 1 datapoint per 20 km radius, yielding 506 data points using the R package spThin[65] to avoid oversampling and the biases associated with community science data. The occurrence data were randomly assorted such that 75% were used to train the model and 25% were used as test data to assess accuracy of the model. 10,000 background points were sampled to establish the environmental domain. This method for establishing background or absence has been found to yield the highest predictive accuracy for Maxent and is uninfluenced by sampling bias.[66,67] Environmental layers were obtained from the WorldClim version 2.1 climate dataset[54] for the period 1970 – 2000 and for the years 2021-2040, based on "worst case scenario" carbon emissions (Shared Socioeconomic Pathway 5-8.5), simulated by NASA's "GISS-E2-1-G" model.[12,13] After filtering out other variables in the dataset that were highly correlated or did not contribute to the model, we used two variables, monthly precipitation and monthly minimum temperature at 30 arcsec spatial resolution. The minimum temperature variable was chosen because cold temperatures are a limiting factor for fungi and cold tolerance determines whether a given species can survive in an area. The variable precipitation was chosen because moisture is another limiting factor for fungal growth and wetting often serves as a signal for mushroom production. We did not include data substrate or other biotic variables in the model and focused on predicting the abiotic component of GOM's niche in North America. For biotic data that may help predict GOM distribution potential, see Figure S5.

The SDM output conveys the relative habitat suitability of areas in North America for GOM given the documented observations used in our training set. Model performance and predictive power were evaluated by the AUC (area under the receiver operating characteristic curve) values which vary from 0 to 1; values < 0.5 indicate that the model performance is worse than random, 0.5 indicates performance that is not better than random, 0.5–0.7 indicates poor performance, 0.7–0.9 indicates reasonable or moderate performance, and >0.9 indicates high performance.[68]

QUANTIFICATION AND STATISTICAL ANALYSIS

Bioinformatics

Illumina amplicon sequence reads were processed using AMPtk v1.6.0.[10] Sequences were de-multiplexed using the unique index combinations and the forward and reverse primers were removed using VSEARCH v2.27.0 Sequences less than 125 bases were discarded and reads greater than 300 bp were trimmed to 300 bp, those less than 300bp were padded with n's. Sequences were

denoised with UNOISE3[69] and subsequently clustered at 97% similarity into operational taxonomic units (OTUs) with VSEARCH. After clustering, we used SynMock to account for observed rates of index bleed using the filtering module of AMPtk. We assigned OTU-level taxonomy using the hybrid taxonomy algorithm in AMPtk based on the UNITE[70] database v9.3 (March 2023) and dropped all non-fungal OTUs from our analysis. Contaminant OTUs identified in control samples were also removed.

Field survey statistical analyses

Analyses were performed in R version 4.2.2[51] using the vegan package v2.6-8.[71] We conducted all following analysis in two ways: 1) by ''tree'', i.e. the combined fungal community from each tree obtained by combining samples from all three heights for each tree, and 2) by ''wood'' i.e. the fungal community from each height of each tree, obtained by sequencing drilled samples from each height independently. Using GOM detection as our independent variable, all analyses tested the differences between tree and wood samples in which we did and did not detect GOM (''with GOM'' and ''without GOM''). We defined GOM detection as molecular detection of GOM sequences in the sample or the presence of GOM basidiocarps anywhere on the tree.

To test for an association between GOM and fungal richness by tree and by wood, we applied a generalized linear model (GLM) with Poisson distribution, appropriate for count data such as species richness, using the glm function in the base R stats package. We made a multivariate GLM using the manyGLM function of the mvabund package[72] with a cutoff value of $p < 0.05$ to test for significant effects of GOM on each detected member of the fungal community in tree and wood samples. To visualize the difference in fungal species richness between samples with and without GOM, we summed the number of unique OTUs in each sample using specnumber. To visualize the fungal communities with and without GOM in ordination space, we first converted the community OTU-read table to occurrence (presence/absence) and calculated a Raup-Crick distance matrix using the raupcrick function,[73] which has proven to be appropriate for zero-weighted datasets. We then visualized the dissimilarity between the communities with nonparametric multidimensional scaling (NMDS) using the metaMDS function.[71] To test whether the presence of GOM influenced the fungal community composition, we performed a nonparametric permutational multivariate ANOVA (PERMANOVA) on our Raup-Crick distance matrix, using the adonis2 function[74] in the vegan package. We first ran the PERMANOVAs including the GOM OTU to match the NMDS visualizations. Next, because the communities in our dataset are labelled by whether they contained GOM, we re-ran PERMANOVAs omitting the GOM OTU to validate that the changes to the rest of the fungal community hold true even without GOM. We analyzed the differences in multivariate dispersion between the groups with and without GOM using the betadisper function[75] in the vegan package on our Raup-Crick distance matrices.

To visualize and compare the ecological guild compositions of the OTUs in trees and wood, with and without GOM, we used FUNGuild[53] version 2.0. We then subset the OTUs that received primary guild assignments of the confidence rankings ''probable'' and ''highly probable'', filtering out ''possible'' and ''unassigned''. Out of 232 total OTUs in trees with GOM (15 trees), we were able to assign probable and highly probable guild assignments to 103 OTUs (44%). Out of 265 total OTUs in trees without GOM (11 trees), 121 OTUs (46%) received probable and highly probable guild assignments. Out of 191 total OTUs in wood with GOM (34 wood samples), we were able to assign probable and highly probable guild assignments to 137 OTUs (46%). Out of 295 total OTUs in wood without GOM (44 wood samples), 151 OTUs (48%) received probable and highly probable guild assignments. Using the curated OTU subsets from trees and wood, with and without GOM, we tallied the occurrence of primary guilds in each tree and wood sample and visualized these data as boxplots. We used Wilcoxon rank sum tests to test for significant differences between trees with and without GOM for each guild and wood with and without GOM for each guild, using the base R stats package.

Current Biology, Volume *35*

Supplemental Information

Invasive golden oyster mushrooms are disrupting native fungal communities as they spread throughout North America

Aishwarya Veerabahu, Mark T. Banik, Daniel L. Lindner, Anne Pringle, and Michelle A. Jusino

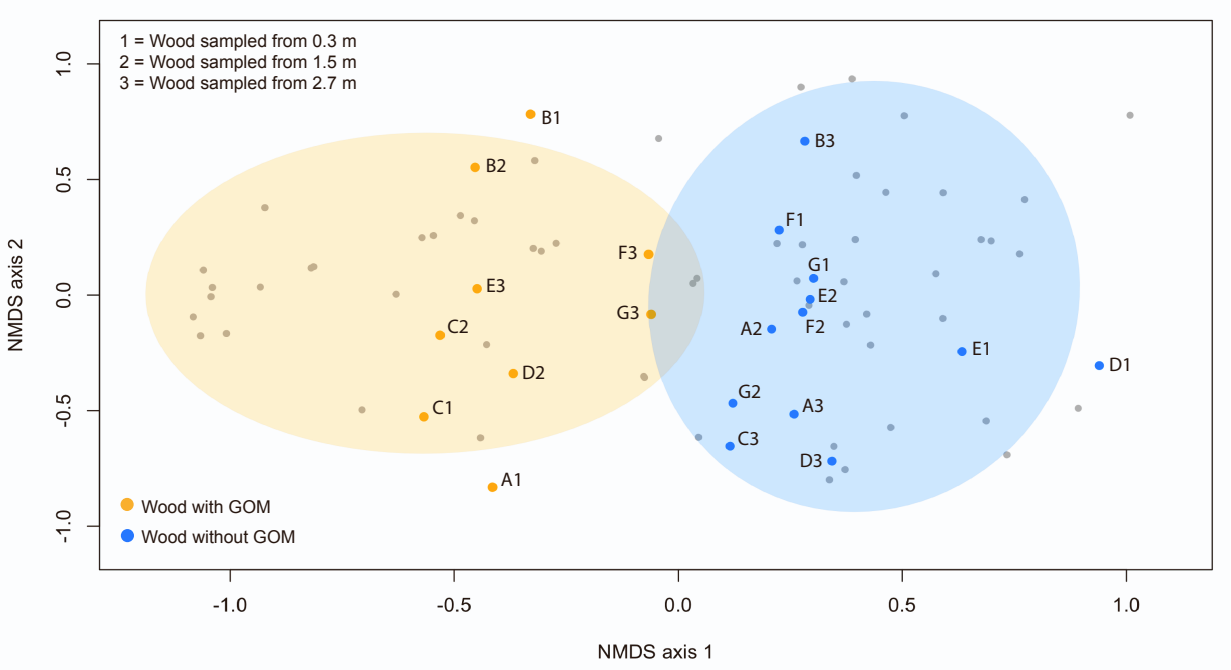

Supplemental Figure 1 – Within partially colonized trees, GOM's impacts on fungal communities appear local and vary by height, related to Figure 3D. NMDS of community compositions in HTAS subsamples taken from wood shavings of seven partially colonized trees, each tree represented by cores drilled at three different heights. Trees labelled with letters (A-G) and heights labelled with numbers (1, 2, 3). Samples from a single tree sort differently if they are with or without GOM, for example, compare B1/B2 to B3 or A1 to A2/A3. Gray dots correspond to all other samples taken from trees in which all cores did or did not have GOM. All points are plotted in the same ordination shown in Fig 2D.

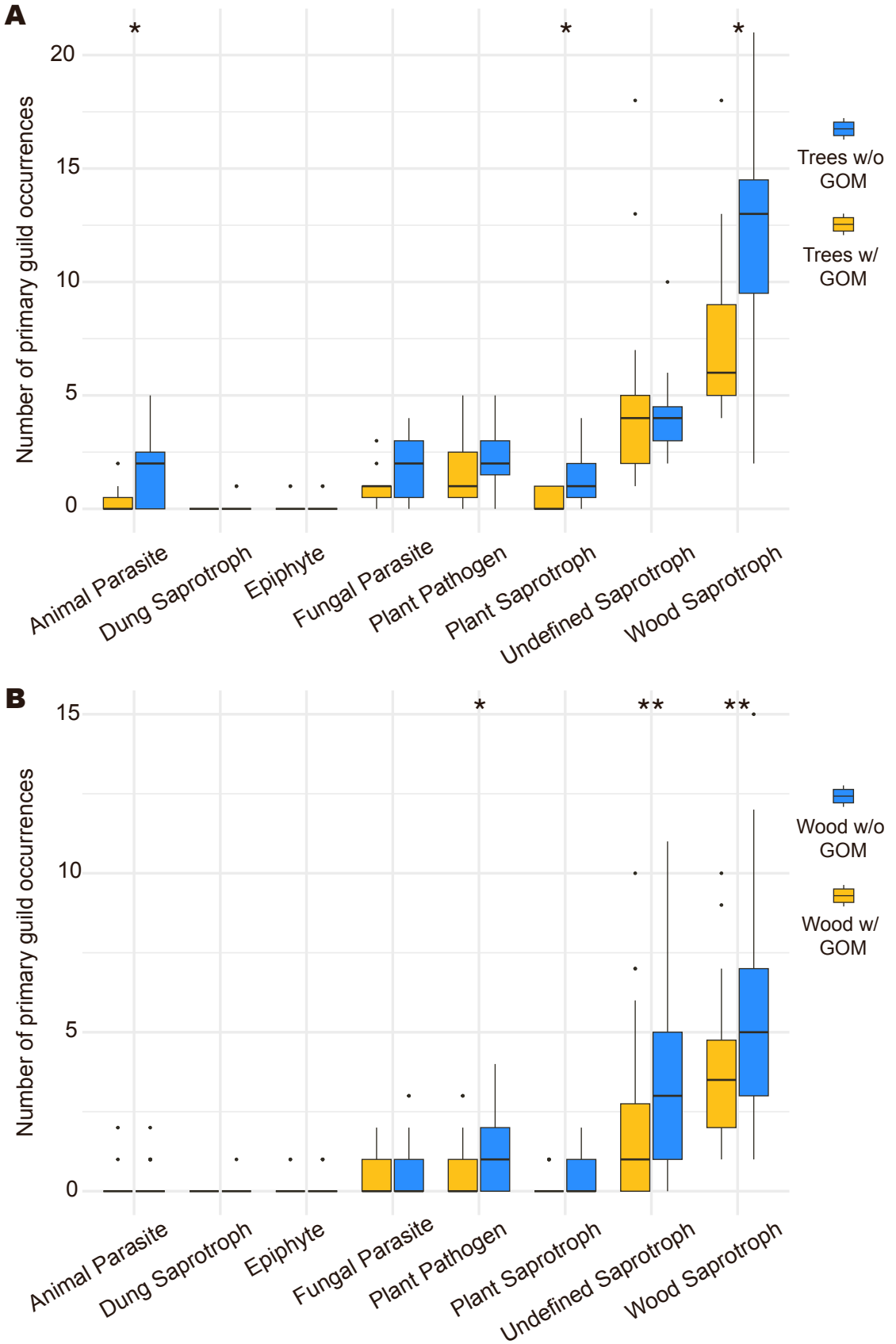
A
Number of primary guild occurrences
20
15
10
5
0
*
*
*
Trees w/o GOM
Trees w/ GOM
Animal Parasite
Dung Saprotroph
Epiphyte
Fungal Parasite
Plant Pathogen
Plant Saprotroph
Undefined Saprotroph
Wood Saprotroph
B
Number of primary guild occurrences
15
10
5
0
*
**
**
Wood w/o GOM
Wood w/ GOM
Animal Parasite
Dung Saprotroph
Epiphyte
Fungal Parasite
Plant Pathogen
Plant Saprotroph
Undefined Saprotroph
Wood Saprotroph

Supplemental Figure 2. Comparison of primary fungal ecological guilds present in trees (A) and wood (B), both with and without GOM. (Related to Figure 2). Boxplots represent the number of occurrences of each primary guild identified by FUNGuild for OTUs with "probable" and "highly probable" guild ranking confidence. In trees with and without GOM, differences between guilds are statistically significant for animal parasites (Wilcox rank sum test: p = 0.015), plant saprotrophs (p = 0.030), and wood saprotrophs (p = 0.033). In wood with and without GOM, differences between guilds are significant for plant pathogens (p = 0.015), undefined saprotrophs (p = 0.002), and wood saprotrophs (p = 0.004).

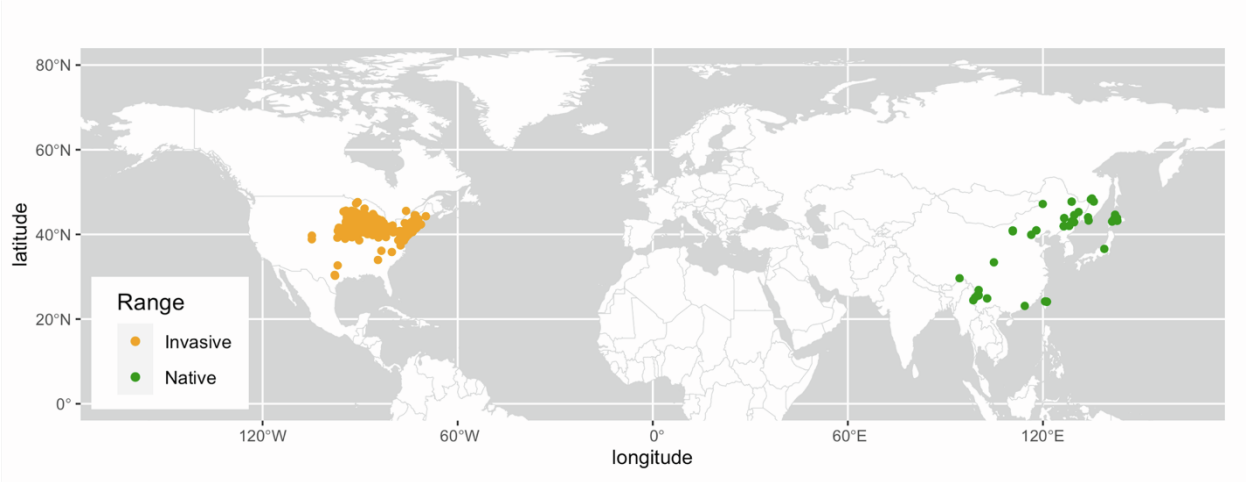

Supplemental Figure 3 – GOM's invasive and native ranges share similarities in latitude, related to Figure 3. World map of GOM's invasive and native ranges. Invasive range observations taken from iNaturalist and MushroomObserver. Native range observations taken from vouchered specimens.

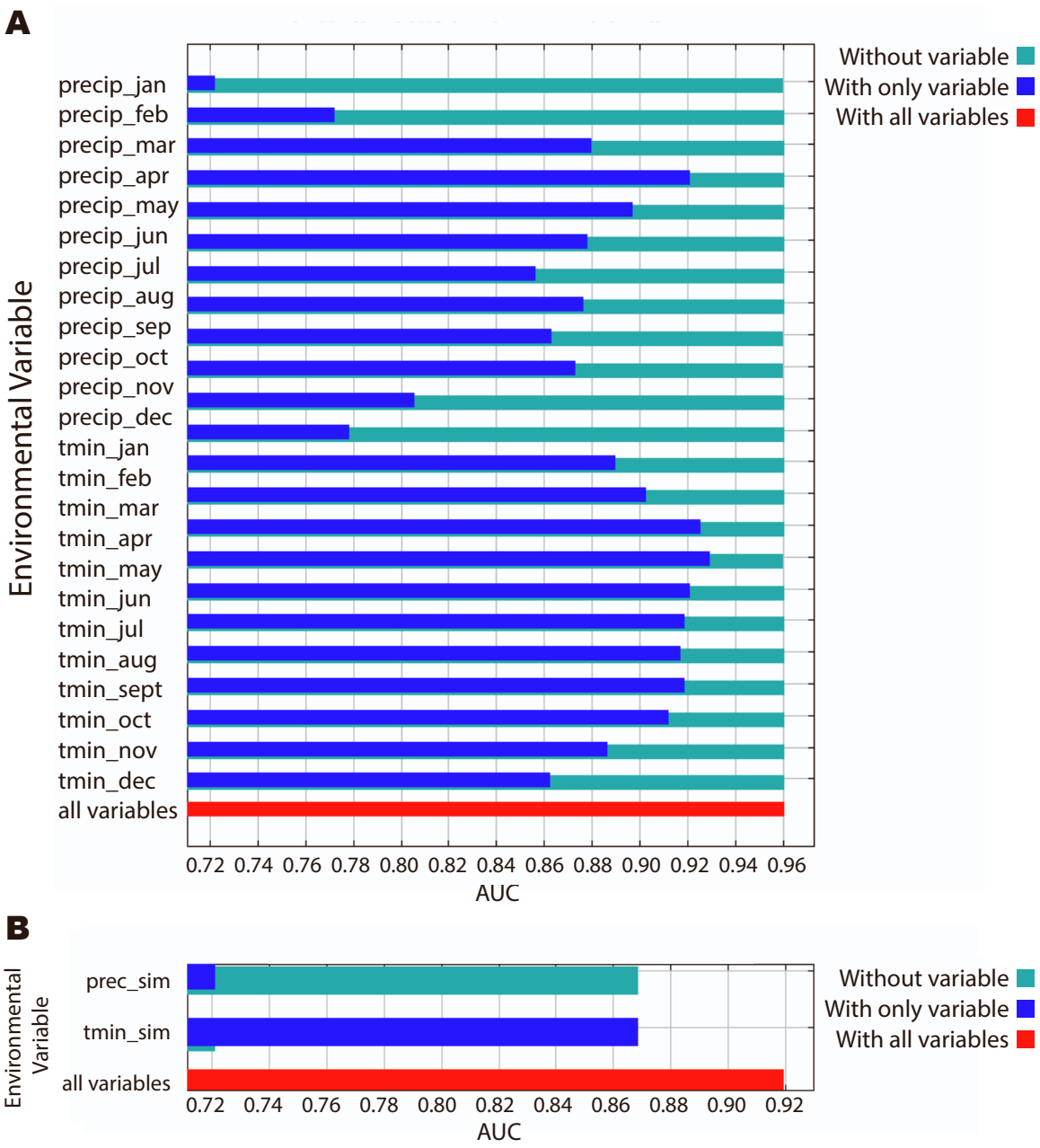

Supplemental Figure 4. Jackknife test results of each environmental variable's contribution towards the performance metric of the model (area under the receiver operating characteristic curve; AUC), for the historical species distribution model (Figure 4A) and the future species distribution model (Figure 4B). "Precip" and "prec" refer to precipitation data, "tmin" refers to minimum temperature data, and "sim" refers to simulated corresponding to the simulated climate data projected for the future.

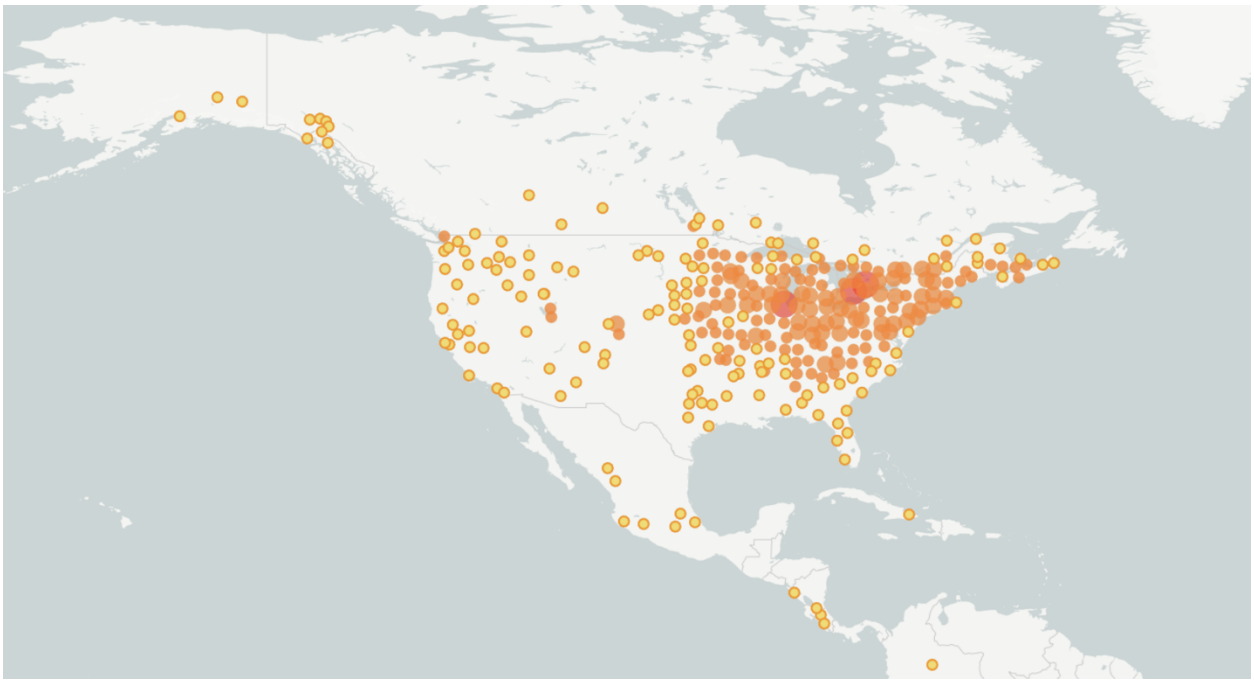

Supplemental Figure 5. North American distribution of *Cerioporus squamosus*, Dryad's Saddle, a native white-rot wood decay fungus often co-occurring with GOM on the same or similar hardwood substrates. (Related to Figure 4.) The full range of substrates GOM can grow on has not yet been documented, but because *C. squamosus* and GOM both grow on multiple hardwood species, the well-documented range of *C. squamosus* is a useful indicator of biotic conditions and forest types where GOM could grow. Such range distributions also help capture fine-scale suitable habitat types (e.g. dead stands at farm edges, parks, riverbanks) that forest inventory data may not include. Data obtained from the GBIF database.

Table 1. Top 5 most common fungal operational taxonomic units (OTUs) detected in 15 trees with golden oyster mushroom (GOM) and 11 trees without GOM. *Because we did not detect a GOM OTU in one tree with a GOM basidiocarp, this value is not 100%.

Top OTUs: Trees w/ GOM	Prevalence	Top OTUs: Trees w/o GOM	Prevalence
Pleurotus citrinopileatus	93.3% *	*Cerrena unicolor*	90.9%
Trichoderma pleuroticola	53.3%	*Trichoderma pleuroticola*	81.8%
Cerioporus squamosus	40%	*Coniochaeta* sp. (LC520183|SH0995824.09FU)	81.8%
Armillaria gallica	40%	*Nemania serpens*	63.6%
Cerrena unicolor	40%	*Phaeocremonium cinereum*	63.6%

Table 2. Fungal operational taxonomic units (OTUs) with decreases of 10% or more in their proportional prevalence in wood with golden oyster mushroom (GOM).

Top OTUs affected by GOM	Species Hypothesis Identifier	Decrease in prevalence
Cerrena unicolor	KM373256|SH1208469.09FU	55.4%
Nemania serpens	AJ390436|SH1033209.09FU	41.4%
Coniochaeta sp.	LC520183|SH0995824.09FU	40.6%
Ascomycota sp.	JQ761901|SH1033209.09FU	35.4%
Phaeocremonium cinereum	KF764561|SH1258358.09FU	33.3%
Trichoderma pleuroticola	EF442083|SH0961555.09FU	25.3%
Phialophora americana	EU514697|SH1280328.09FU	24.2%
Scytalidium cuboideum	FN812780|SH1276408.09FU	24.2%
Exophiala sp.	LC317596|SH1266707.09FU	20.6%
Cylindroconidiis aquaticus	MH236576|SH1040511.09FU	20.4%
Chaetothyriales sp.	KT265803|SH1254406.09FU	20.0%
Calocera sp.	KP013031|SH0995592.09FU	20.0%
Coniochaeta sp.	UDB0399909|SH0906001.09FU	19.2%
Helotiales sp.	AY557369|SH1276173.09FU	18.4%
Trichoderma sp.	AY154947|SH0961555.09FU	18.0%
Helotiales sp.	KF800131|SH1276173.09FU	17.8%
Herpotrichiellaceae sp.	EU041811|SH1089749.09FU	17.8%
Colacogloea cycloclastica	KX611018|SH0906051.09FU	15.6%
Nemania sp.	OM262247|SH1033209.09FU	15.6%
Cadophora novi-eboraci	MW804701|SH0963000.09FU	14.7%
Flabellascus tenuirostris	KT716469|SH1329526.09FU	14.7%
Dactylospora sp.	KF274260|SH1023760.09FU	13.9%
Sistotrema brinkmanii	DQ899094|SH1208561.09FU	13.3%
Ceratostomella pyrenaica	KT991672|SH1110604.09FU	13.3%
Leotiomycetes sp.	KY689631|SH0975632.09FU	13.3%
Ascomycota sp.	KF274260|SH1023760.09FU	13.3%
Phleogena faginae	MK564583|SH1321020.09FU	12.5%
Entocybe sp.	AB907595|SH1111501.09FU	11.1%
Niesslia sp.	UDB02241807|SH1078366.09FU	11.1%
Hypsizygus ulmarius	LC096110|SH1086718.09FU	10.3%
Graphium sp.	MH283080|SH0987501.09FU	10.3%
Helotiaceae sp.	UDB0244624|SH0962969.09FU	10.3%
Biatriospora sp.	UDB01513575|SH0992953.09FU	10.3%